NSG-724

Informal Interim Report No 3

EXPERIMENTAL INVESTIGATION OF

STAGNATION POINT ELECTRODES

GPO PRICE $ _____

CFSTI PRICE(S) $ _____

by

Hard copy (HC) _2.00_

Michael Chen and E. Zimet

Microfiche (MF) _.50_

ff 653 July 65

DEPARTMENT OF ENGINEERING

AND APPLIED SCIENCE

YALE UNIVERSITY

I. INTRODUCTION

While considerable progress has been made in recent years in application of ionized gases, one of the least understood areas remains that of the interaction of an electrode with a relatively dense, partially ionized plasma. The problem is of obvious interest to magnetohydrodynamics, electrical propulsion, and high temperature test facility development. Due to the multiplicity of the physical processes involved, and the poor quantitative understanding of these "component" processes, it is not even clear which ones of the many simultaneous processes and competing influences were dominant. As a result, theoretical models often differ from each other in fundamental assumptions. It is clear that in this circumstance it is desirable if not necessary to begin with experimental observations under realistic conditions.

Unfortunately, the electrode processes for high pressure discharges are characteristically unstable and non-reproducible. Even in the rare instances where relatively stable discharges were obtained, the severe non-uniformities and asymmetry almost invariably preclude meaningful, space resolved data. The majority of existing experimental measurements thus consist mainly of gross measurements of total current, voltage, and heat transfer. Even such important parameter as the local electrode surface temperature versus local current density, and the state of the plasma adjacent to the electrode are generally not known with certainty. In view of the complexity of the physical processes involved, these gross measurements are in general insufficient to provide either significant insight to the problem, or unequivocal means to evaluate hypothetical theoretical models.

In order to alleviate some of these problems and to provide space resolved steady state data under realistic and relatively controllable conditions, measurements have been carried out for an experimental electrode placed in the stagnation flow of a separately controlled, arc heated plasma. As there existed no theoretical study of sufficient thoroughness to either serve as a guideline or to provide incentive for verification, the experimental emphases were placed on: (1) seeking a configuration which would yield a stable, reproducible discharge, and (2) obtaining as much correlatable and space resolved data as possible.

The experimental set up is shown in Figures 1a, 1b, and 1c. Bottled gas is heated in a converging diverging nozzle by a steady state coaxial arc discharge employing the nozzle as anode and a pointed cathode in the subsonic side of the nozzle. The resulting plasma jet impinges on the experimental electrode forming successively a normal shock and an aerodynamic boundary layer. The experimental electrode is independently biased with respect to the plasma outside the boundary layer, whose potential was monitored with a reference probe downstream of the experimental electrode. Spectroscopic measurements of the plasma, radiometric measurements of the electrode surface, and electrode current voltage characteristics were obtained simultaneously for different plasma conditions. Due to the unavoidable radial gradients of the small Reynold number nozzle flow, no calorimetric data was attempted. The details of these experiments will be described in later sections.

The choice of the experimental configuration was prompted by the following considerations:

1. In the usual electrode experiments, the plasma environment was maintained by the same discharge under study, thus it was difficult to separate the influences of the plasma properties versus the electrode properties. To overcome this problem, the plasma should be generated separately and be separately controlled.

2. It was felt desirable to take advantage of the aerodynamic boundary layer so that the electrode influences are confined in a small, fairly well defined region. In this respect the stagnation flow boundary layer, possessing uniform thickness and uniform heat and species fluxes is particularly advantageous. If the electrical conductivity of the external plasma is much higher than in the boundary layer, the discharge under investigation can be considered to take place between the experimental electrode and a parallel "virtual electrode" consisting of the plasma outside the boundary layer. It was intended to use the apparatus for both cathode and anode studies. Since rafractory cathode operation is expected to depend on solid heat conduction processes which have very slow time constants, this requirement rules out shock tube or other non-steady techniques.

3. The need for spectroscopic mapping of the plasma environment made it desirable to have radially symmetric external flow over the electrode so that Abel inversion could be used to obtain local intensities.

4. Some early pyrometric surface temperature measurements were complicated by plasma radiation. The capability for completely mapping the plasma radiation field would eliminate this uncertainty.

5. It was postulated that the discharge constriction near the electrode might be caused by an inherent instability rather than non-uniformity of the imposed conditions and geometry. The uniform plasma environment attainable with the stagnation point configuration appeared to provide a means to test this theory.

As evidenced by the data presented below, the experimental arrangement fulfilled these expectations, and steady state, uniform discharges were obtained with no more than the usual experimental difficulties. However, in view of the lack of theoretical understanding of the operating parameters, no attempt has been made to optimize the apparatus. Instead, emphasis was plased on exploiting the current capabilities to gather as much data as can be meaningfully obtained at this time. It is hoped that after these data are fully analyzed, one would be in a better position to judge what would be the most fruitful improvement.

A. GENERAL CONDITIONS

The arc heater-nozzle had a throat diameter of 0.100 inch. No attempt was made todiagnose the flow except immediately upstream of the experimental electrode.

The argon flow rate was varied between .05 and 1.25 scfm. The arc heater current could be varied between 20 Amp and 120 Amps. The lower current represented the marginal current below which the heater became unstable[4] and electrical and aerodynamic oscillations could be observed.

While spotty data have been obtained for a much wider range of conditions, most of the data presented below were obtained in one of four conditions.

This was due to the fact that spectroscopic measurements with the large quantities of required data represented an almost overwhelming burden for the personnel available. The four conditions are listed in Table 1.

Gas Heater		Argon Flow		Stagnation pressure	Specific Power Input
Amps	Volts	sc+m	gm/sec	mmHg	joules/gm
40	26	0.45	3.35×10^{-2}	40	3.10×10^{4}
40	26	0.68	5.06×10^{-2}	40	2.06×10^{4}
80	23	0.45	3.35×10^{-2}	40	5.49×10^{4}
80	23	0.68	5.06×10^{-2}	40	3.64×10^{4}

B. ELECTRICAL CHARACTERISTICS OF THE ELECTRODE

As shown in Fig. 1, the electrode consists of a 1/8 inch diameter 2% thoriated tungsten rod which has been mounted flush within a 3/8 inch boron nitride insulating tube. Due to a suspected chemical reaction, the inside diameter of the boron nitride was enlarged 0.020 inches about the 1/8 inch tungsten rod 1/4 inch back from the tip of the electrode. For the remaining length of the electrode, about 6 inches, the tungsten and boron nitride were in physical contact.

The second electrode seen in the figure is a reference probe from which the test electrode potentials were measured. This was also sheathed in boron nitride so that only the front surface was electrically active: A constant 0.5 mA electron current was drawn for all tests, to provide a relatively constant reference potential. No correction was made for the plasma potential or ambipolar field. The uncertainty and error was expected to be insignificant.

The electrode data may be discussed in terms of three operating modes; as an anode, as a cathode at low currents, and as a cathode at higher currents. Fig. 2-6 are the anode characteristics for varying stagnation pressure and

nozzle conditions. It is seen that although stagnation pressure has some effect, the characteristics are fairly independent of power and flow rate input to the nozzle especially at low currents. Also, it is seen that none of these curves are linear in a semi-log plot so that one cannot interpret the slope in terms of an electron temperature from the simple relationships available for probes. At no time was an electron saturation level reached.

The second condition, that of small currents to a cathode, is shown in Fig. 7. At these small currents, the cathode may be considered to act as a probe, and the curves exhibit an ion saturation. Unlike the anode condition, a fairly strong dependence upon the power input to the nozzle is noted.

Letting

$$j_+ = eM_{+\infty} \frac{\overline{v}_+}{4} \tag{1}$$

where j_+ is the ion saturation current, $M_{+\infty}$ the number density of ions in the undisturbed plasma, and $\overline{v}_+$ an average thermal velocity which for a Maxwellian distribution is $(8kT_+/\pi m_+)^{\frac{1}{2}}$, one may estimate the order of magnitude of $n_{+\infty}$. From these data using 2000°K and 10,000°K as lower and upper bounds of the ion temperature. These results are shown in the following table:

TABLE 2   Estimated Ion Densities

	T°K	$n_{+\infty}/cm^3$
40 Amp runs	2,000	$1.8 (10)^{14}$
	10,000	$8 (10)^{13}$
80 Amp runs	2,000	$1. (10)^{15}$
	10,000	$4.8 (10)^{14}$

Note that the spectroscopy results yielded an excitation temperature of the order of 10,000°K, which corresponds to an ion density of about $5(10)^{14}/cm^3$. The Stark broadening also yielded electron densities of this order of magnitude.

As the voltage to the cathode is increased, a slight increase in current is noted in Figs. 8-11. At some voltage generally of the order of 200 volts, the cathode breaks down to a thermionic emission mode with a corresponding drop in voltage. For new cathodes, the discharge was relatively unstable. For an unknown reason, cathodes which had been operated several times previously appeared to be much more stable, setting into a uniform, steady discharge in about 10 seconds. Hence, the curves shown represent values obtained with a "used" cathodes. Figures 10 and 11 which represent higher power input to the nozzle show that the transition to the emitting mode is quite smooth, and that there is little gap between the two modes. In general, this was not true of the lower power input curves, Fig. 8 and 9, in which higher voltages were required to induce breakdown. However, once the cathode reached the emitting state, the values for all four curves were quite similar, and all have roughly the same slope.

C. ELECTRODE SURFACE TEMPERATURES

The electrode tip temperature was determined by measuring the emitted radiation from the electrode and computing the temperature from Planck's law of radiation.

$$E_{\lambda b} = C_1 \; \lambda^{-5}/(e^{c_2/\lambda T} - 1)^{-1} \tag{2}$$

Two mirrors were positioned so that the tip could be viewed spectro-scopically even though the body of the electrode was encased in boron nitride. The resulting configuration was calibrated with a standard spectral lamp.

To remove any ambiguity caused by plasma radiation as opposed to electrode radiation, the radiation was measured at a wavelength well away from any argon lines. In principle, plasma radiation could be measured first and then subtracted from the surface radiation. In practice, this was deemed unnecessary in terms of the measured intensities. As a further check of plasma radiation, the current to the electrode was then turned on and off and the time dependent intensity of the electrode was recorded. By extrapolating these heating and cooling curves, it was found that the plasma contribution was negligable. As mentioned, the electrode behavior was found to change initially with usage, so that the values reported again represent that of a "used" elec-trode. Due to the degree of surface roughness obtained by the electrode, a black body emission was assumed. This would tend to underestimate tempera-tures.

Figures 12-14 show these measured temperatures as a function of current for both anode and cathode. A fairly linear dependence is noted in both cases, with the cathode temperature being less sensitive to current than the anode.

Based on the equation of thermal emission

$$j = AT^2 e^{-\phi e/kT} \tag{3}$$

an effective value of ϕ was computed for the measured cathode temperatures using a value of $A = 60.2$ amp/cm^2 K^2. Since no corrections were made for field

effects and other emission mechanisms, this value does not represent the true work function. It is of interest to note that the value of $\phi = 3.3v$ corresponds quite closely to that of thorium.

D. SPECTROSCOPIC RESULTS

Spectral results were obtained utilizing a 0.5 meter Jarrell Ash monochrometer mounted upon a motor driven traversing table. In this manner spatial scans were obtained without the need for moving the plasma jet. The instrument was focused and the position of the electrode tip relative to the entrance slit was ascertained by the following procedure. A lamp was placed behind the electrode, and the shadow of the electrode was cast upon the entrance slits. The monochrometer was then adjusted so that a light intensity versus an axial position scan would show a transition from the intensity of the lamp to a relative zero intensity in a distance corresponding to the resolution of the optical system. For the results presented, this width was 0.005 inches, and hence the position of the slit relative to the electrode could be determined to this accuracy. The plasma intensity was compared to that of a standard spectral lamp which was placed at the same position as the plasma jet so that it was seen through the same optics.

The radial traverse intensity scans obtained were Abel inverted by fitting a polynomial to the data points and then differentiating and integrating analytically. This was done on an IBM 7094 computer. Over sixty points were taken per scan to reduce the inherent inaccuracy caused by the differentiation.

Since the Abel inversion is based upon an optical depth of zero, i.e., there should be no significant absorption and the Abel inversion was utilized

in reducing the data, it was felt that some justification of this assumption would be merited.

Seven ArI lines were selected on the basis of relative strengths and the availability of transition probability data [5,6,7]. These lines were then used to obtain radial intensity traverses for two conditions. The first condition was a normal scan, in the second condition a mirror was placed behind the jet so that light emitted in the opposite direction to the monochrometer would also be observed. Clearly, if the plasma is transparent, and the reflectivity of the mirror is considered, one should get twice the intensity for the mirror condition as one would get without the mirror. On the basis of the above experiment, four lines were chosen as to be relatively free of absorption.

A very important consideration to be taken in making spectroscopic temperature determinations is that of local thermodynamic equilibrium. In the expression

$$I(\omega) = 1/4\pi \ A_{mn} \ h\omega \ \frac{Ng_n}{Z} \ e^{-e_n/kT} \tag{4}$$

the inverted intensity is related to transition probability, wave number, and number density of the emitting species. For the Boltzmann relationship to hold, equilibrium must be obtained. If equilibrium does exist, the same temperature distribution should be obtained when different lines are used. Figures 16-19 show the temperature distribution for four lines for a plane .002" away from the electrode. It was felt that these temperatures were too high in that electron density results from Stark broadening corresponded to lower values. However, it is interesting to note that these temperatures are in agreement among themselves.

Similar spectroscopic data for different planes in front of the cathode have been obtained for a wide range of conditions. Except for the planes immediately adjacent to the electrode, the data cannot be converted to temperatures, due to the lack of local pressure data. Plots of the intensities, however, are useful in indicating the distribution of excited state population. A typical curve is shown in Fig. 20.

In view of the high gradients in the vicinity of the electrode, it is not likely that equilibrium can be satisfied. Indeed, some of the intensities obtained were found to be higher than the maximum allowed under equilibrium considerations.

The spectroscopic data obtained to date are by no means complete, and more extensive measurements will be undertaken.

E.   STARK BROADENING

The final measurements made to date are those of electron densities by the Stark broadening of the hydrogen beta line. These measurements were obtained by mixing 1% of hydrogen into the argon jet. Scans were than taken for six wavelengths at three different electrode conditions. These curves were then inverted, and the points obtained were fitted to a calculated line profile[8]. From the half width of these curves the electron densities were obtained.

For both the cathode and anode condition at 10 amperes the electron densities were roughly the same, 1.0×10^{15} electrons/cm^3. For the condition of zero current the electron density was about half of this value.

F. DISCUSSIONS

The above results demonstrated that detailed, space resolved measurements of either the plasma or solid observables could be made for an electrode operating in a dense, flowing plasma. While the measurements were by no means complete, these data probably represented the first detailed investigations under steady state, controllable conditions. As a result, they clearly raised more questions than they answered.

In reviewing these results, there have been strong temptations to offer theoretical explanations for the observed trends, as well as experimental schemes to clarify one or two specific effects. Such attempts would probably be inopportune at this moment due to a poor understanding of the overall picture. Efforts for more detailed measurements are currently being continued.

REFERENCES

1. Ecker, G., Ergebn. d. exakt. Naturw. _33_, pp. 1-104 (1961).

2. Chen, M. M., "Some Elementary Considerations Concerning the Uniformity of Electrical Conduction Through Gases", VIIth Sym. on Engineering Aspects of Magnetohydrodynamics, Princeton, N. J., March 30, April 1, 1966.

   See also "Characteristics and Stability of a Self-sustained Thermionic Cathode", Informal Interim Report No. 1, NASA Grant 724, prepared by M. M. Chen, Yale University, April 1966, and "Fundamental Conditions for Uniform Current Distribution in a Medium with Temperature Dependent Conductivity", Informal Interim Report No. 2, Grant 724, prepared by M. M. Chen, April 1966.

3. "Experimental and Theoretical Research on Plasma Sheaths and Boundary Layers Around Stagnation Point Electrodes", semi-annual Progress Report No. 1, Jan. 1965, Grant NASA-NSG-724, submitted by Yale University.

4. As above, Report No. 2.

5. Olsen, H. N., J. Quant. Spectrosc. Radint. Transfer., Vol. 3, pp. 59-76, 1963.

6. Adcock, B. D. and Plumtree, J. Q., S. RT. Vol. 4, pp. 29-39, 1964.

7. Popenol, C. H., Shumaker, Jr., J. B., Journal of Research N.B.S., Vol. 69A, No. 6, (1965).

8. Griem, H. R., Plasma Spectroscopy, McGraw-Hill, 1964.

FIGURES

NOT TO SCALE

SUPERSONIC ARC-HEATED NOZZLE & TEST ELECTRODE
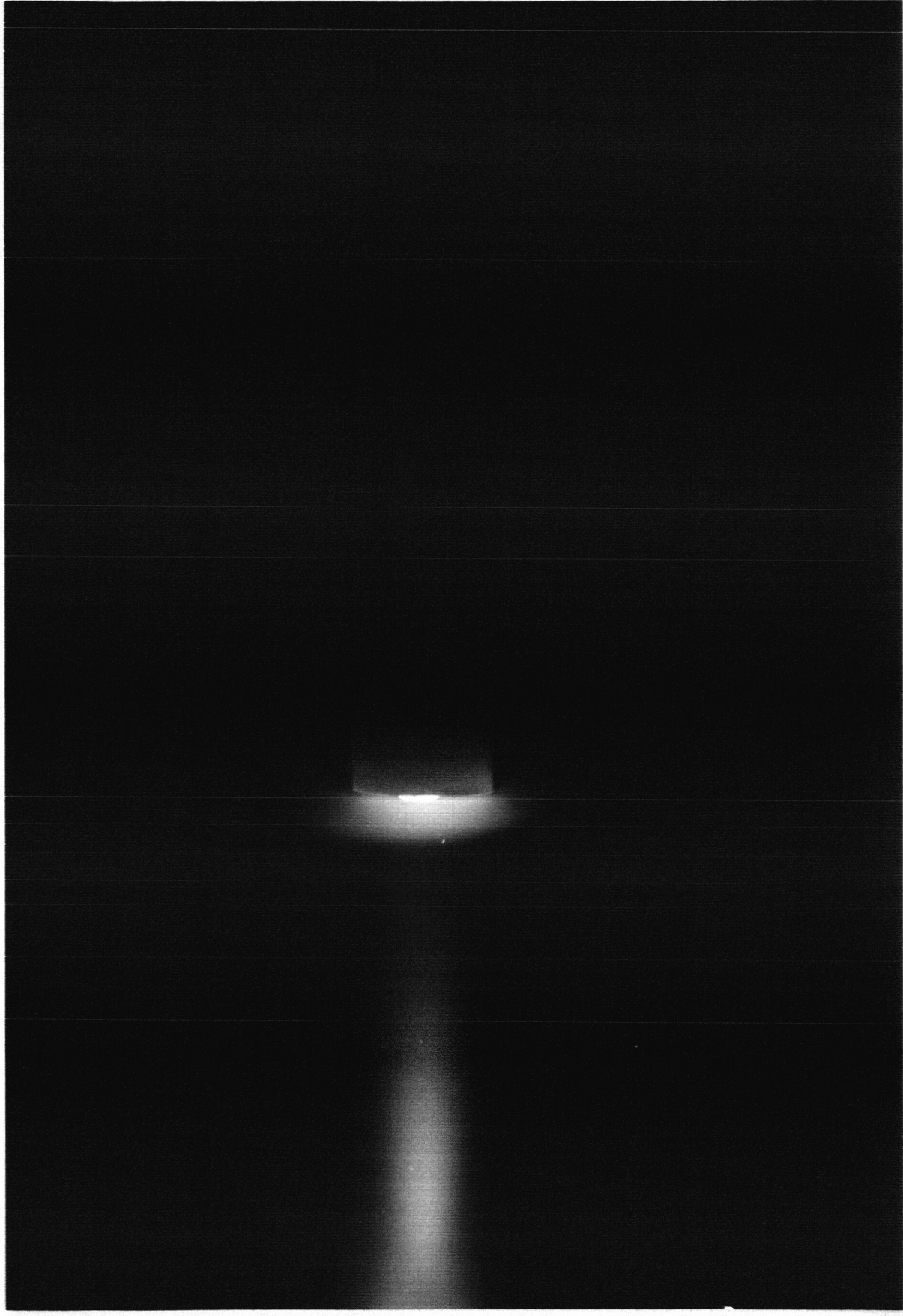
FIGURE I

TEST ELECTRODE AND REFERENCE PROBE

FIGURE 1B

BATTERY POWER
EXCEPT STARTING CIRCUIT

REVERSIBLE POLARITY
220 OR 440 VOLTS

TEST ELECTRODE

REFERENCE PROBE

90 V   180 K Ω

NOZZLE

220 VOLTS

ARC STARTING CIRCUIT

7Ω

7Ω

220 VOLTS

FIGURE IC

ANODE
CURRENT VS. VOLTAGE

40. AMPS
26 VOLTS
0.45 CFM

STAGNATION PRESSURE   7. 75 MM HG

AMPERES

VOLTS

FIGURE 2

80 AMPS
23 VOLTS

0.45 CFM

STAGNATION PRESSURE 40.0 MM HG
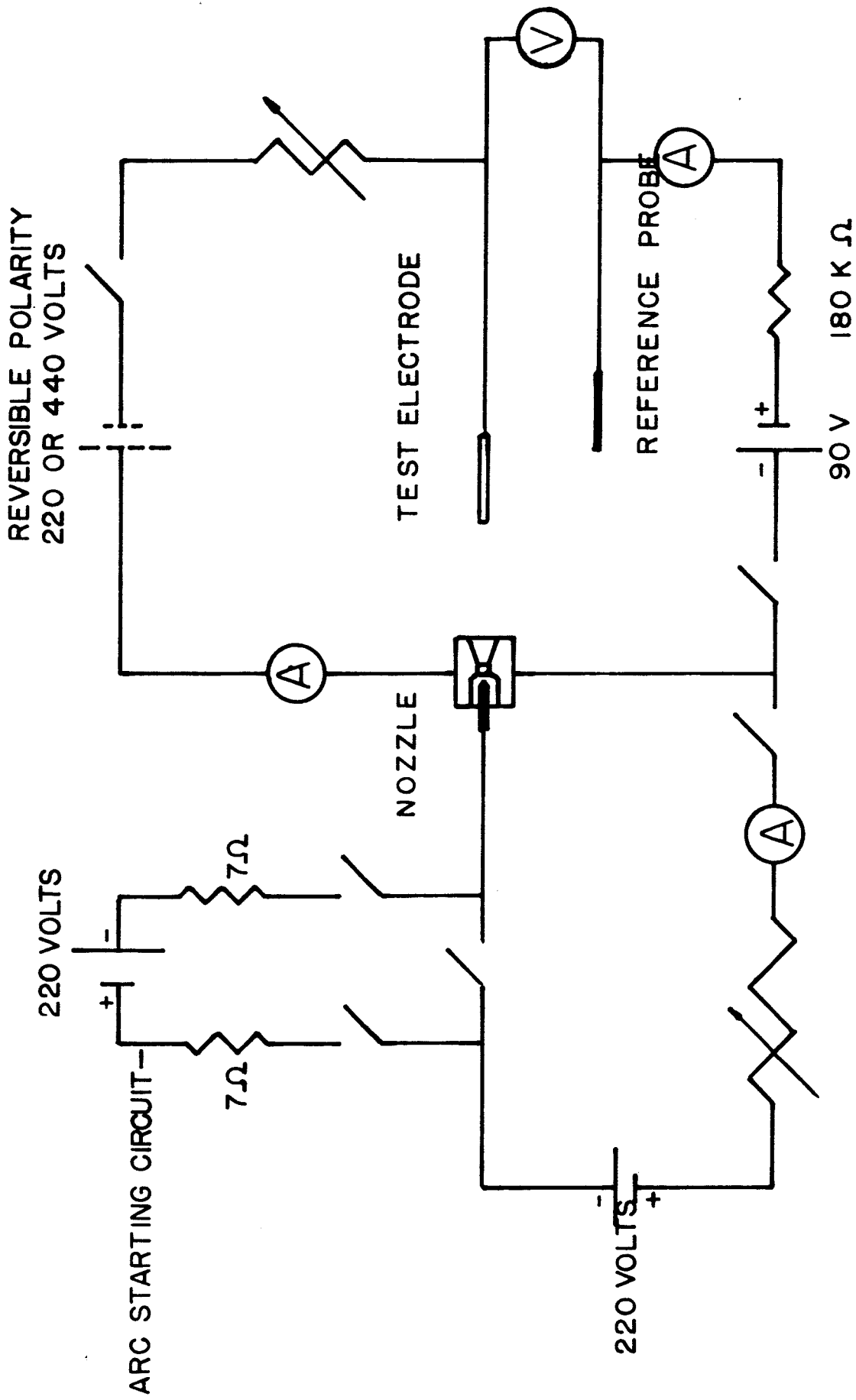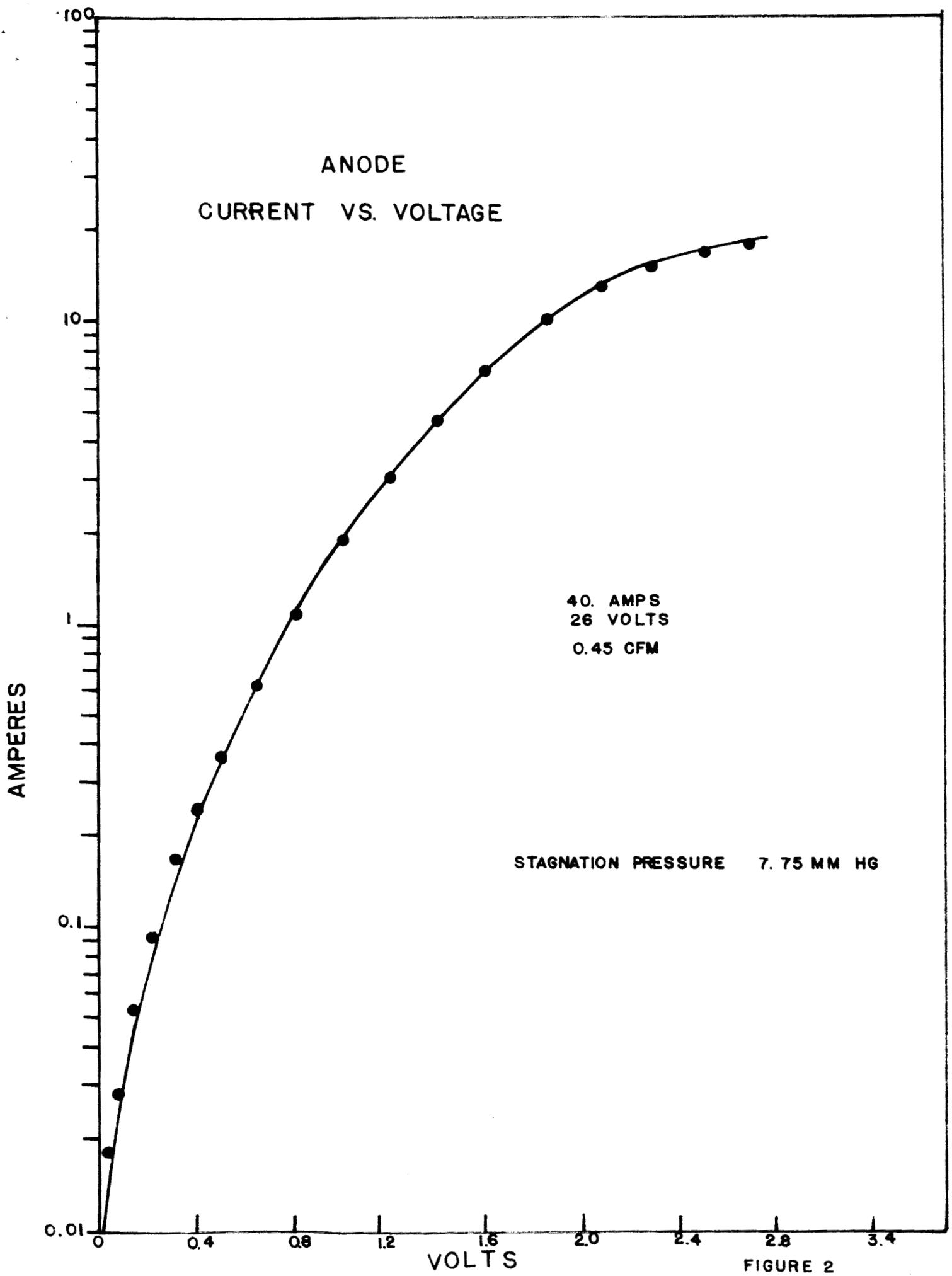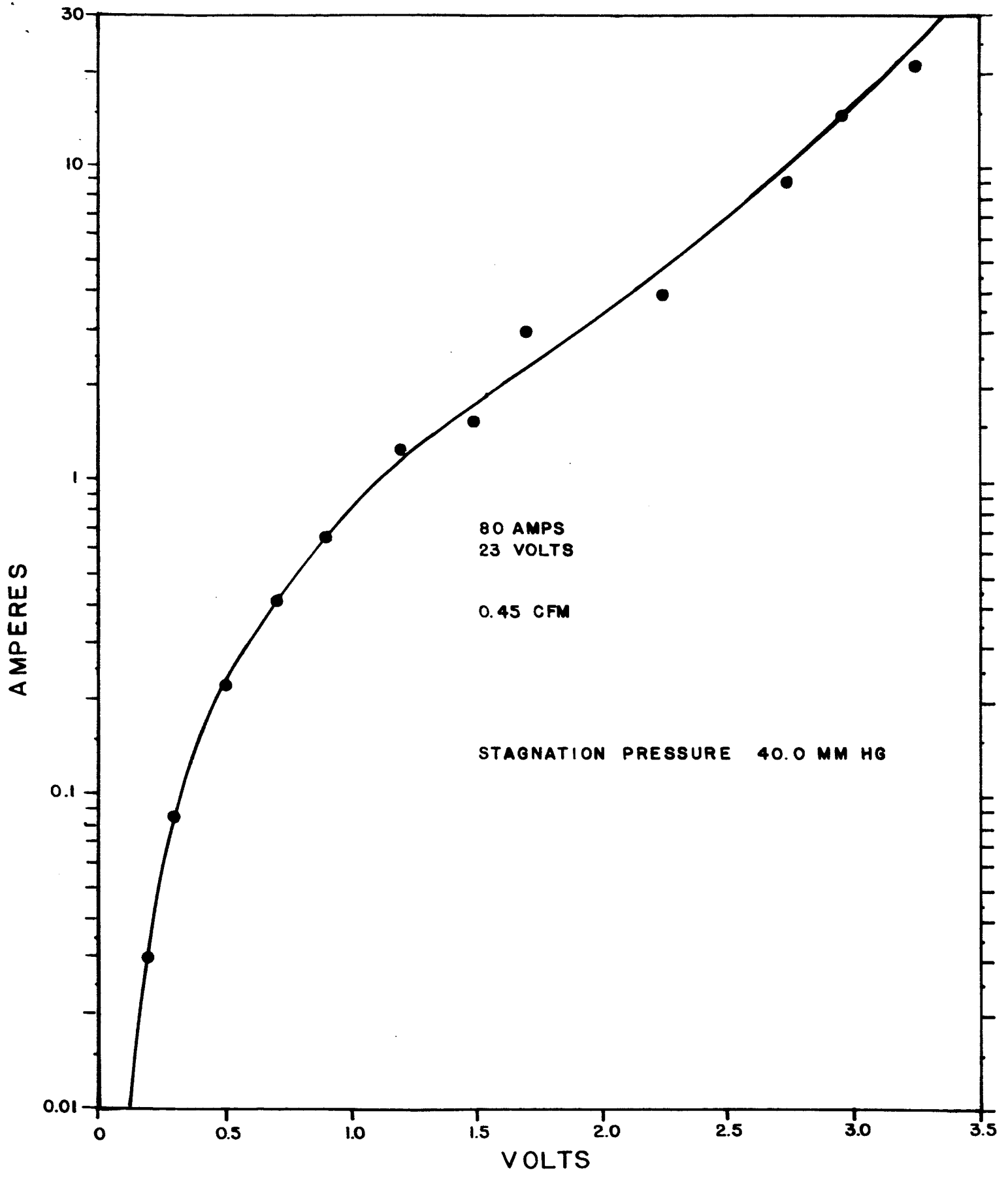
ANODE CURRENT VS. VOLTAGE
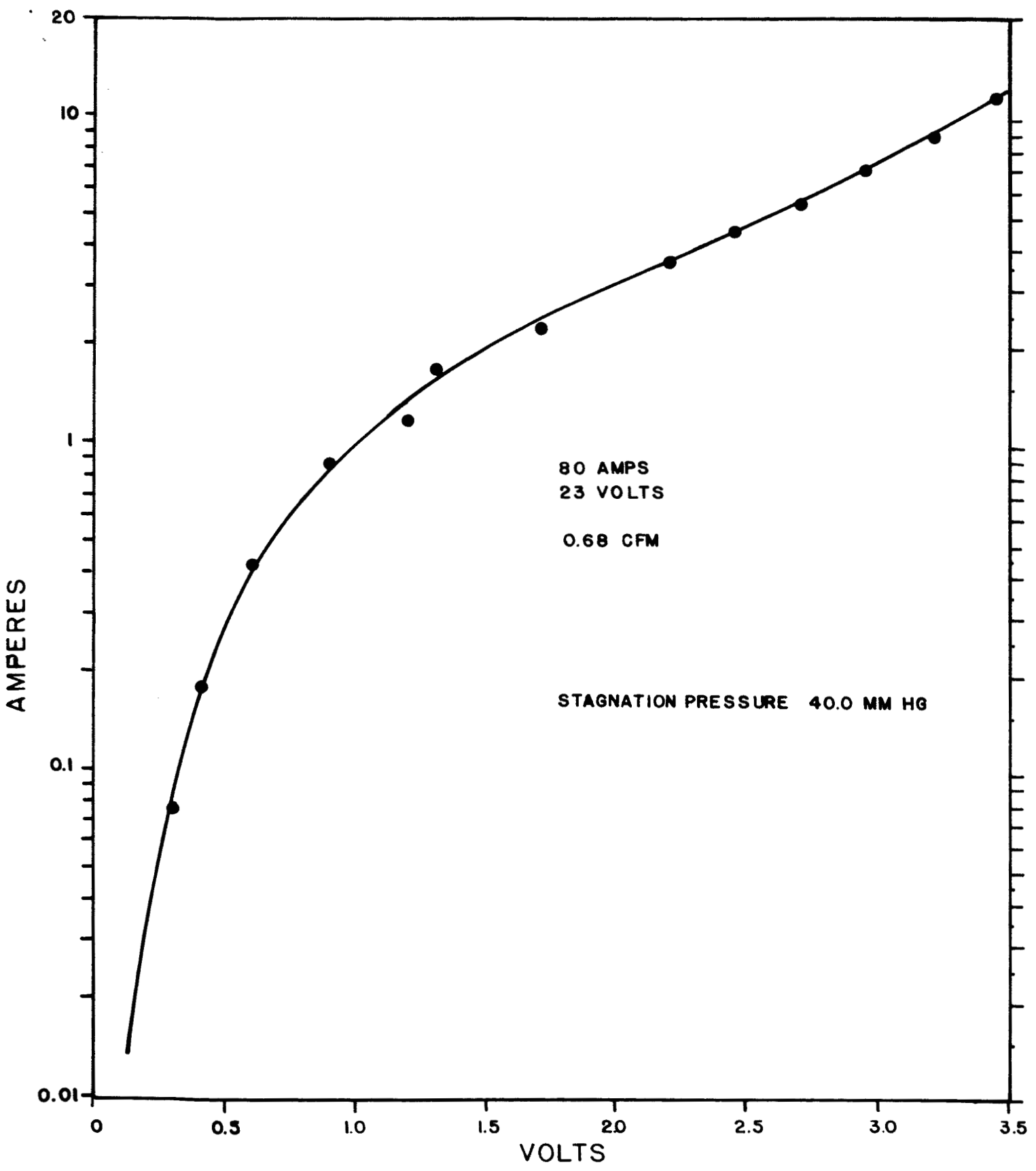
FIGURE 3

ANODE CURRENT VS. VOLTAGE

FIGURE 4
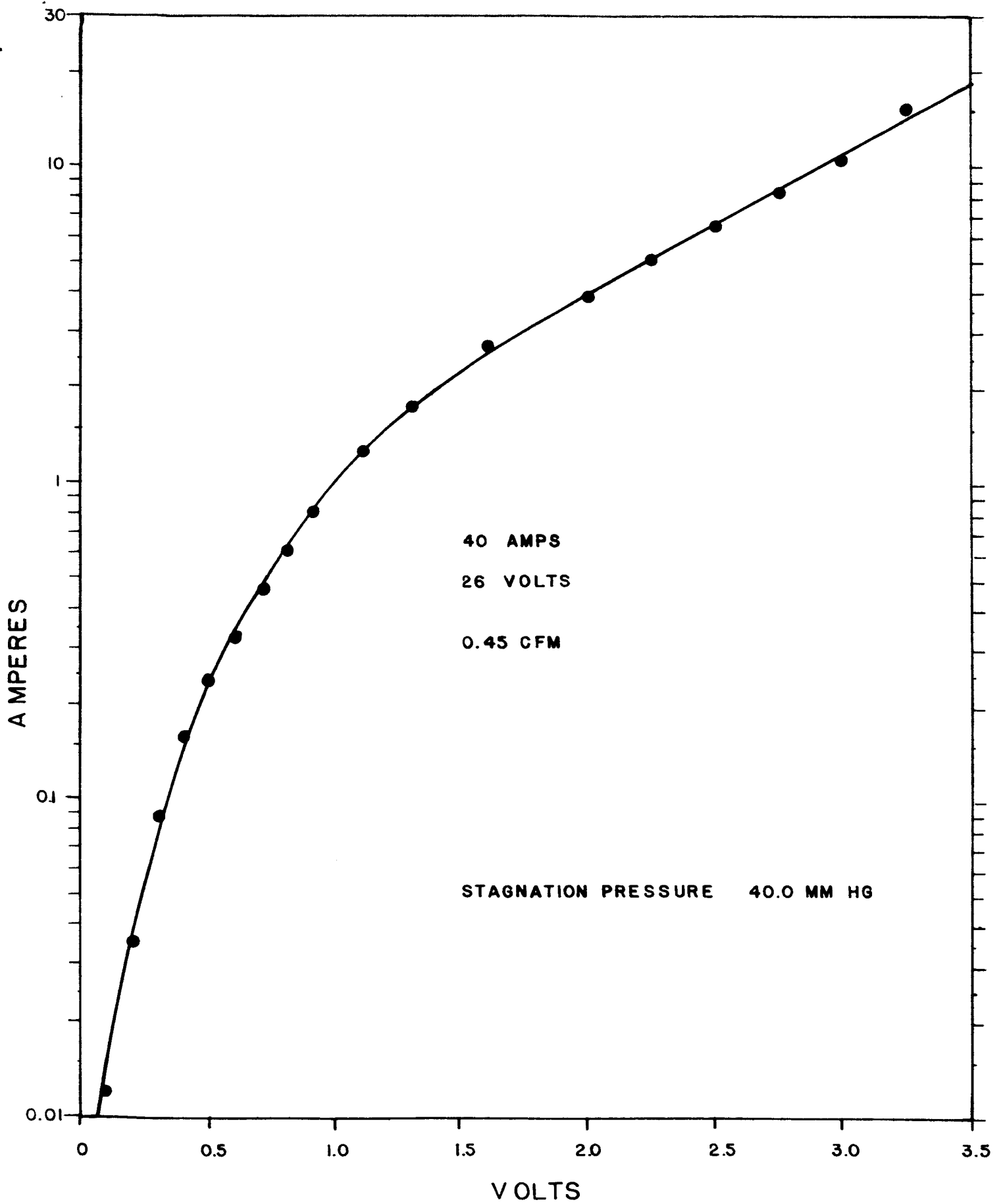
ANODE CURRENT VS. VOLTAGE

FIGURE 5
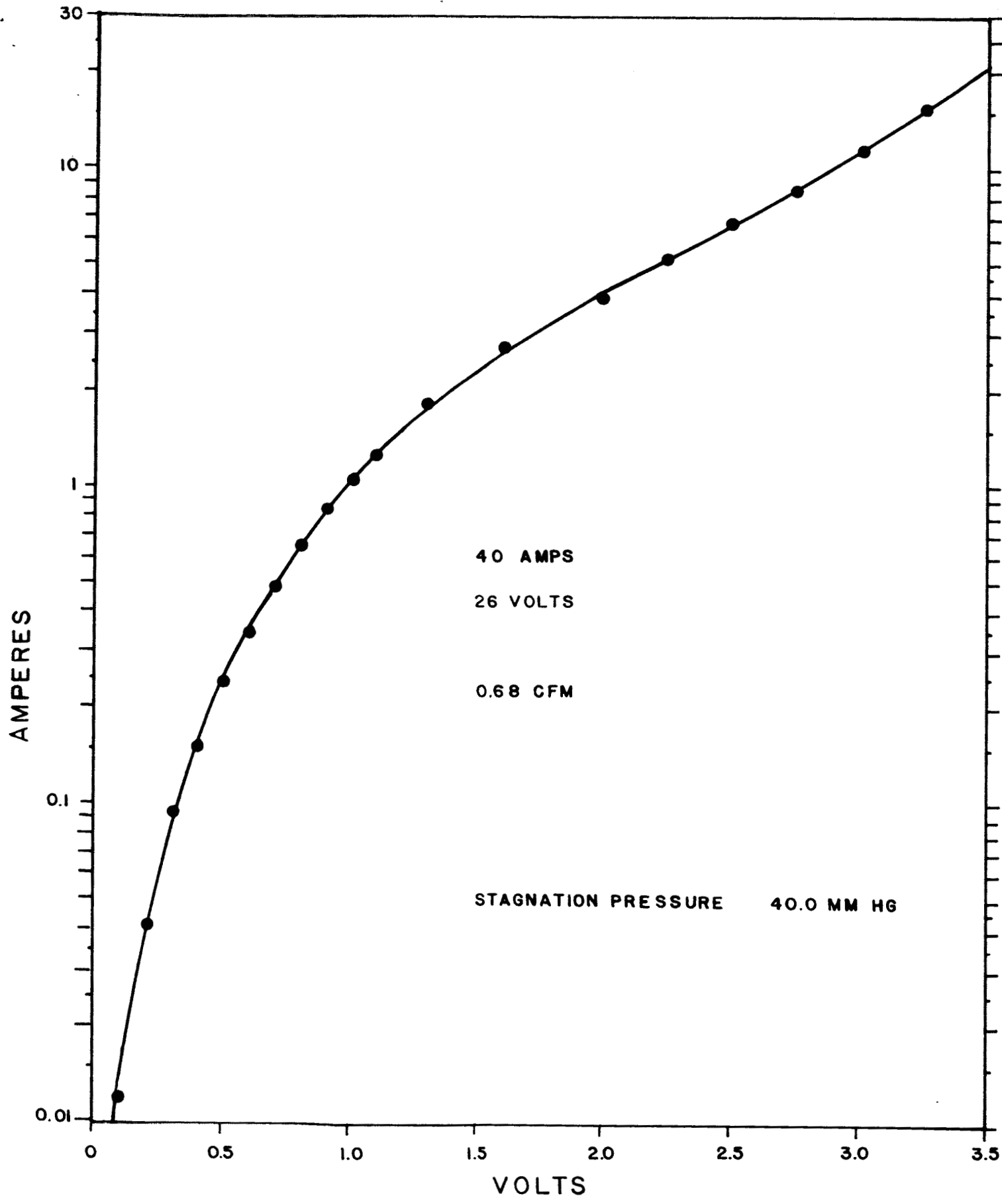
ANODE CURRENT VS. VOLTAGE

FIGURE 6

CATHODE CURRENT VS. VOLTAGE

FIGURE 7

80 AMPS

23 VOLTS

0.45 CFM

STAGNATION PRESSURE   40.0 MM HG
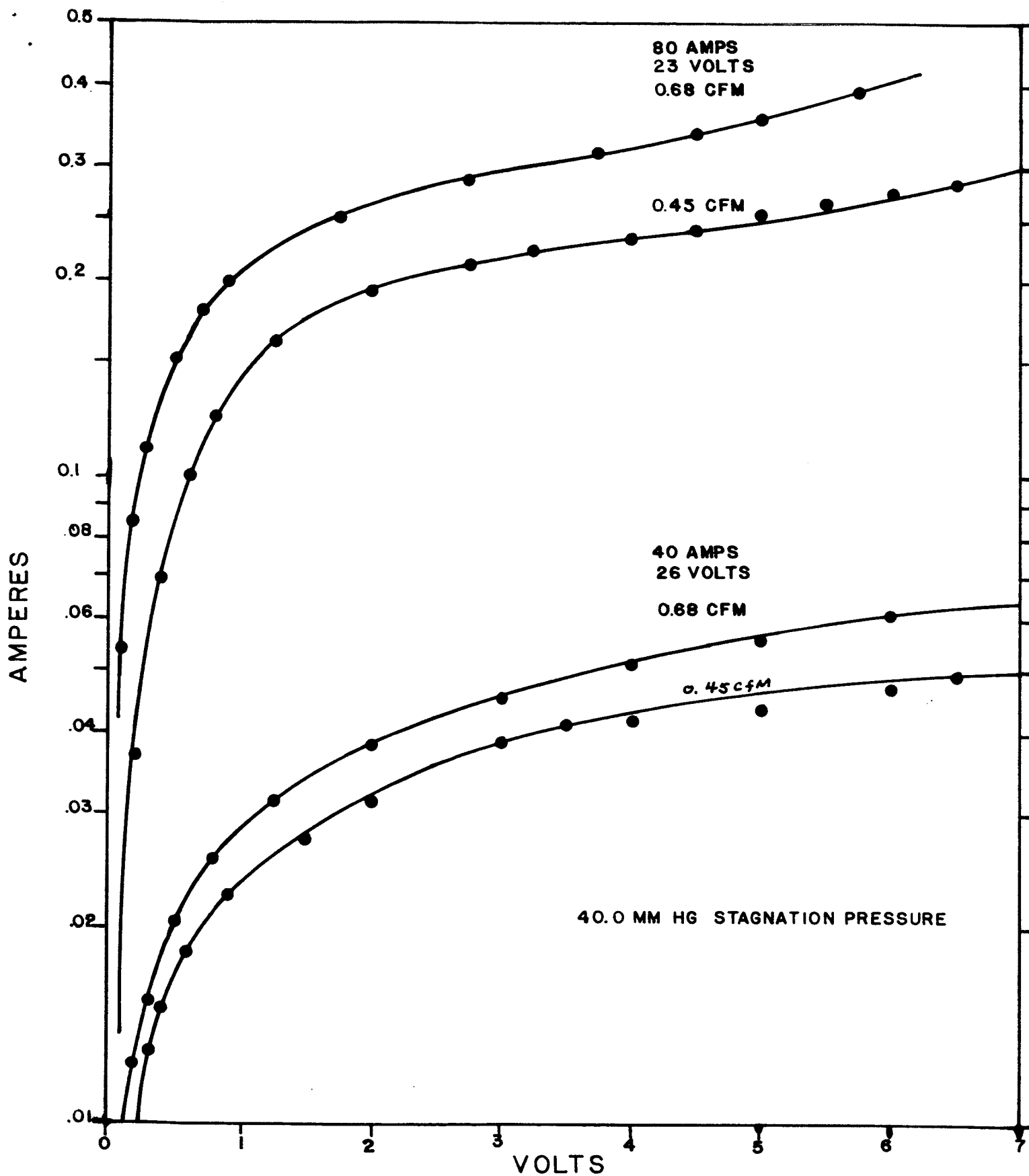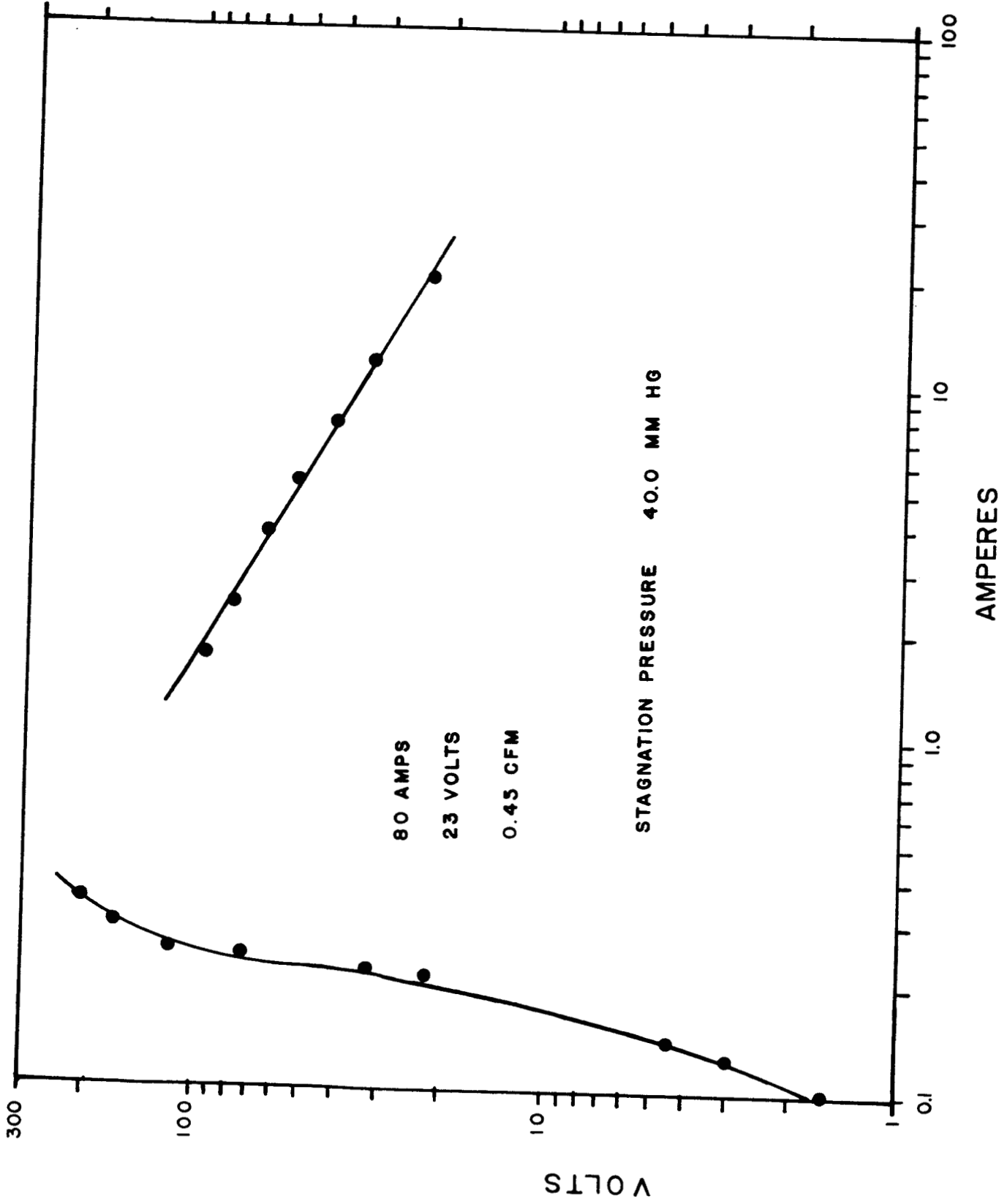
CATHODE VOLTAGE VS. CURRENT

FIGURE 8

CATHODE VOLTAGE VS. CURRENT

FIGURE 9
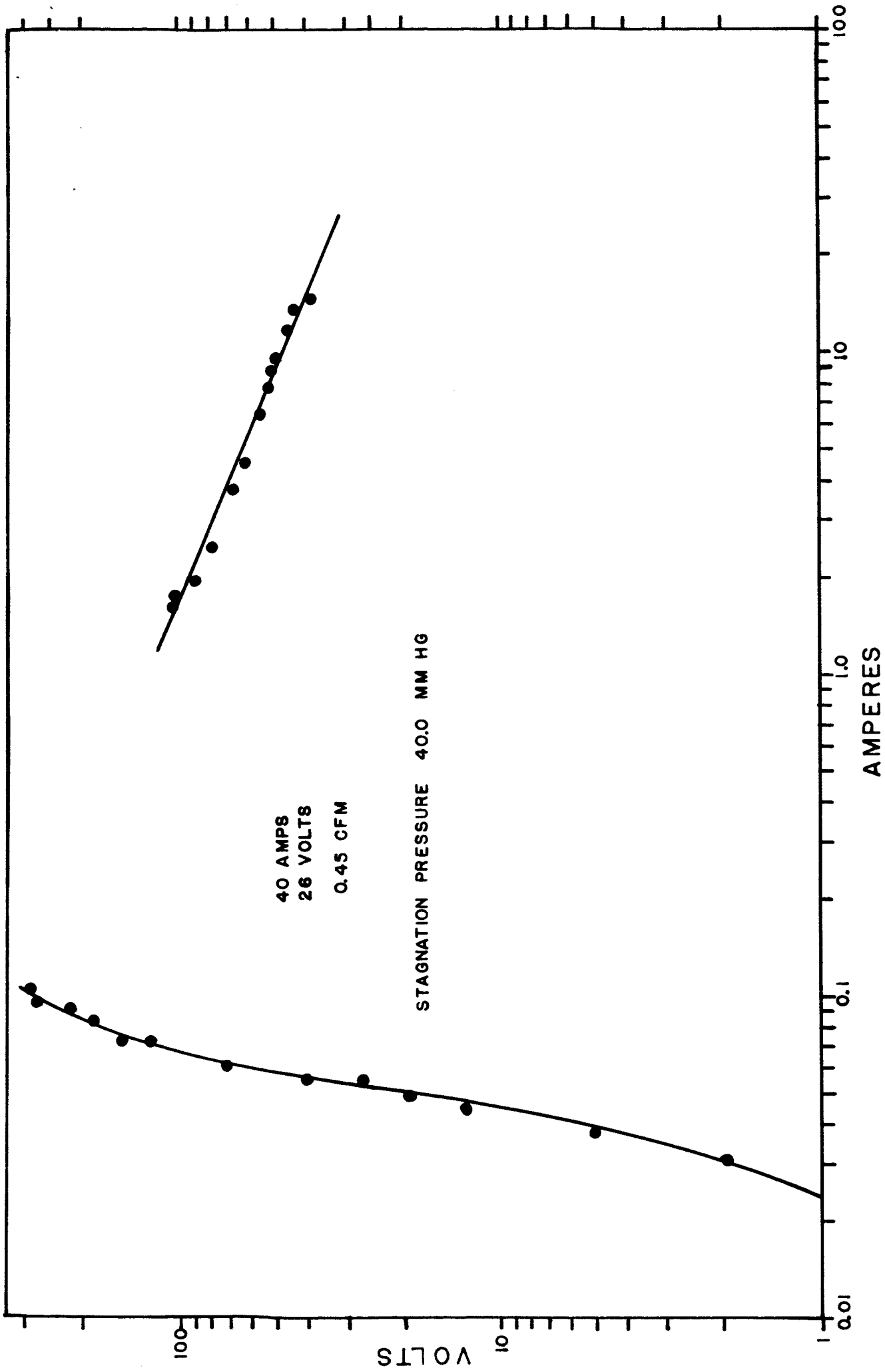
VOLTS

AMPERES

80 AMPS

23 VOLTS

0.68 CFM

STAGNATION PRESSURE 40.0 MM HG

40 AMPS
26 VOLTS

0.45 CFM

STAGNATION PRESSURE 40.0 MM HG

AMPERES

CATHODE VOLTAGE VS. CURRENT

FIGURE 10

40 AMPS
26 VOLTS
0.68 CFM

STAGNATION PRESSURE 40.0 MM HG
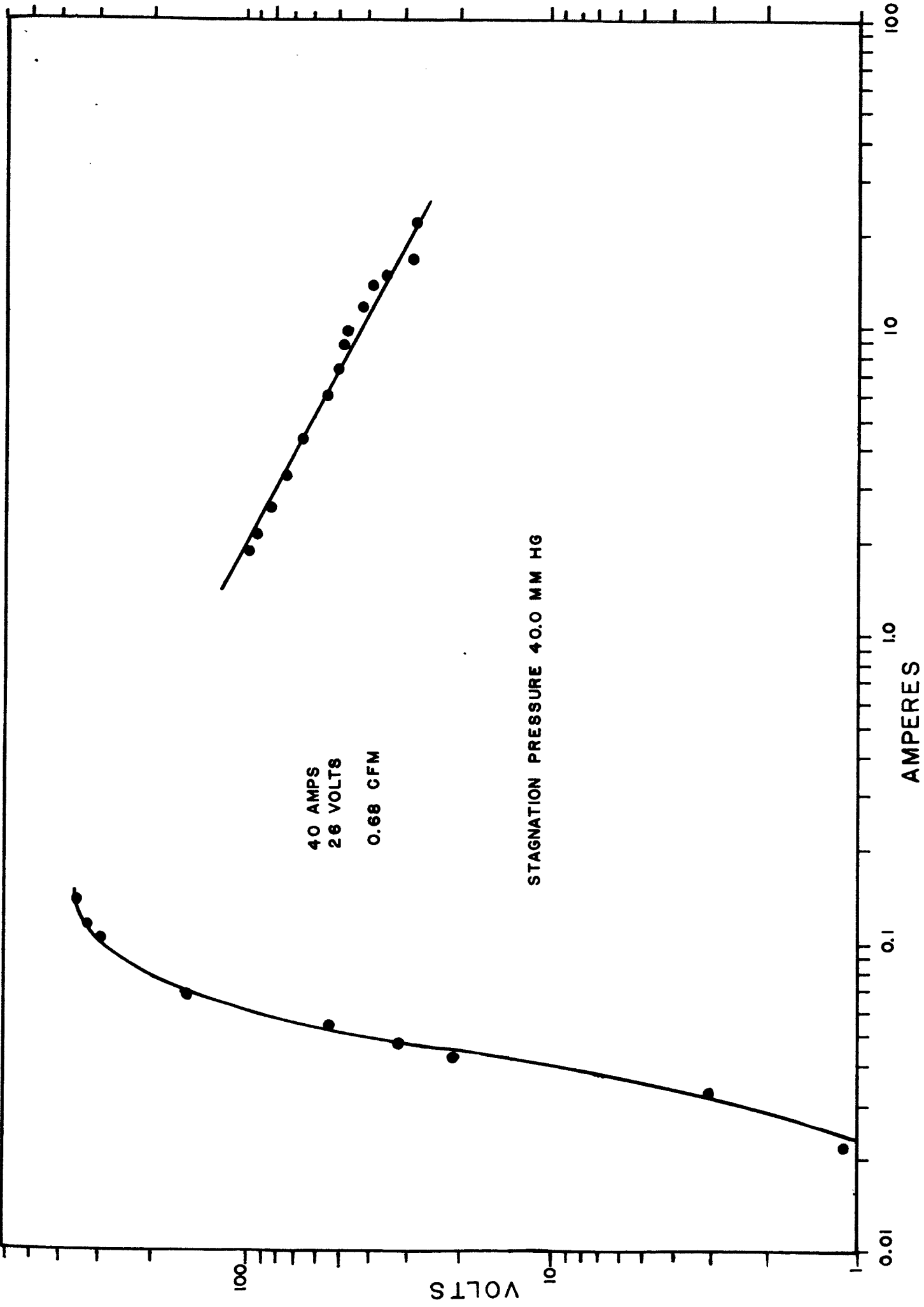
CATHODE VOLTAGE VS. CURRENT
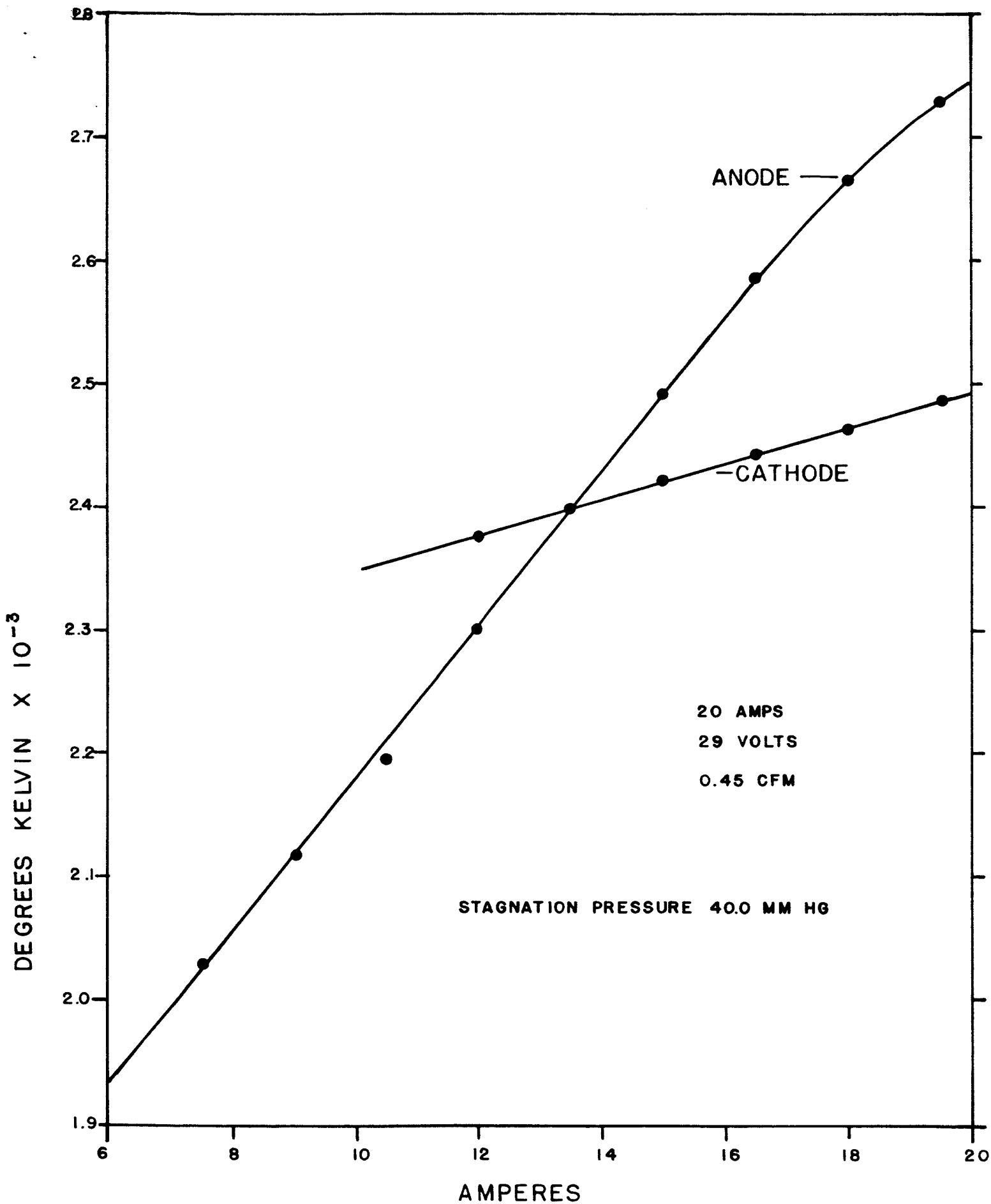
FIGURE II

TEMPERATURE VS. CURRENT TO ELECTRODE
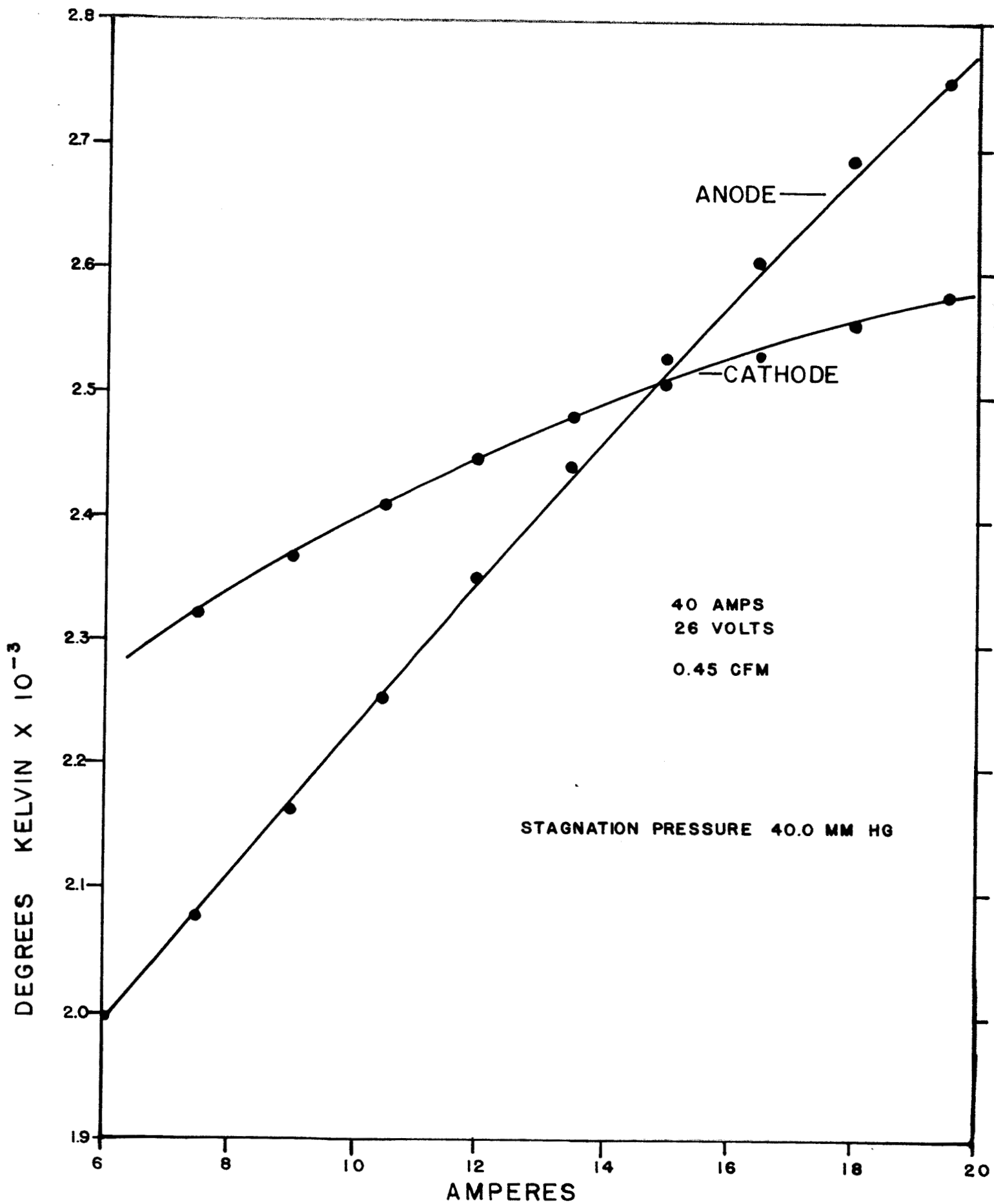
FIGURE 12

TEMPERATURE VS. CURRENT TO ELECTRODE
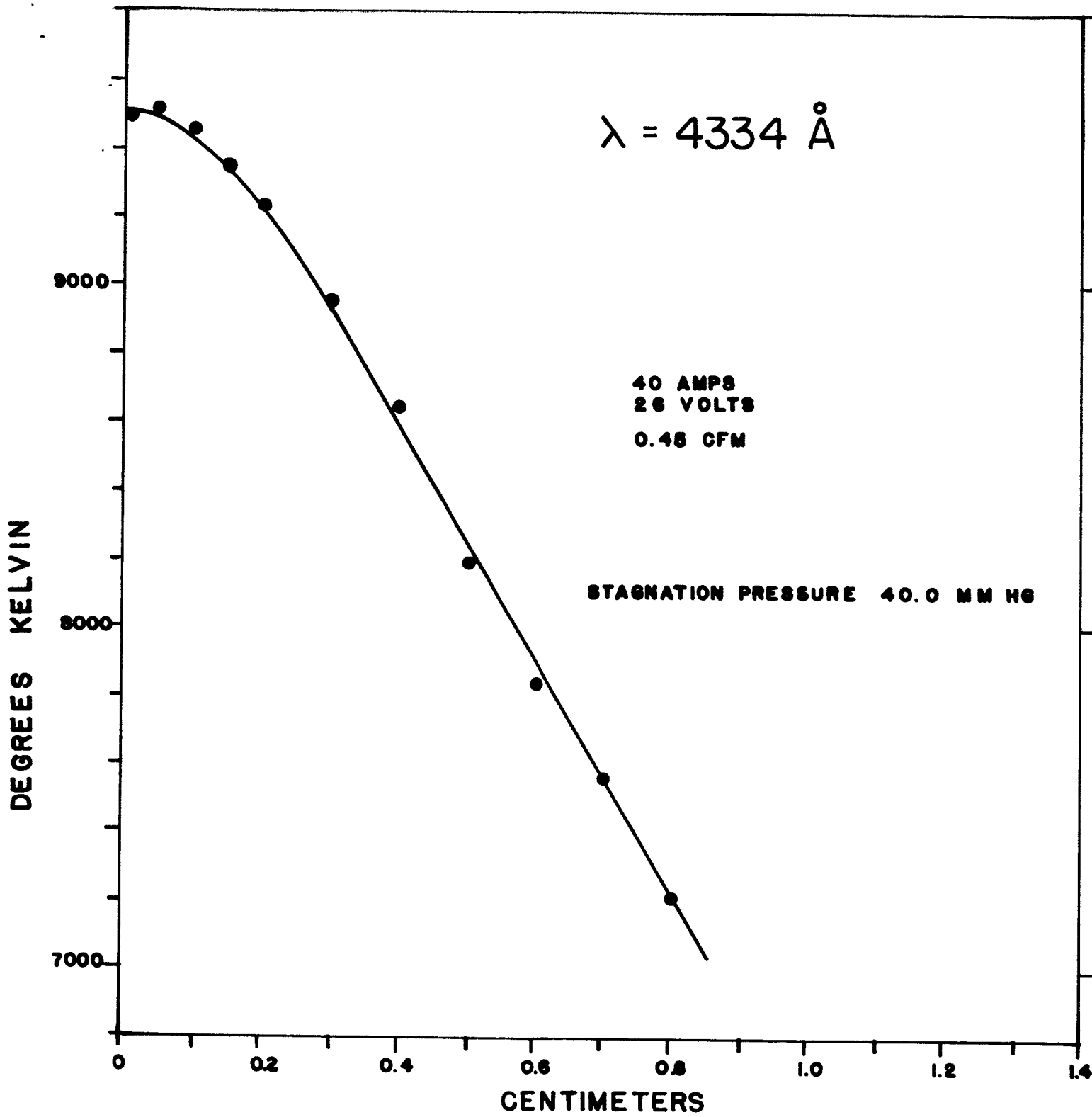
FIGURE 13
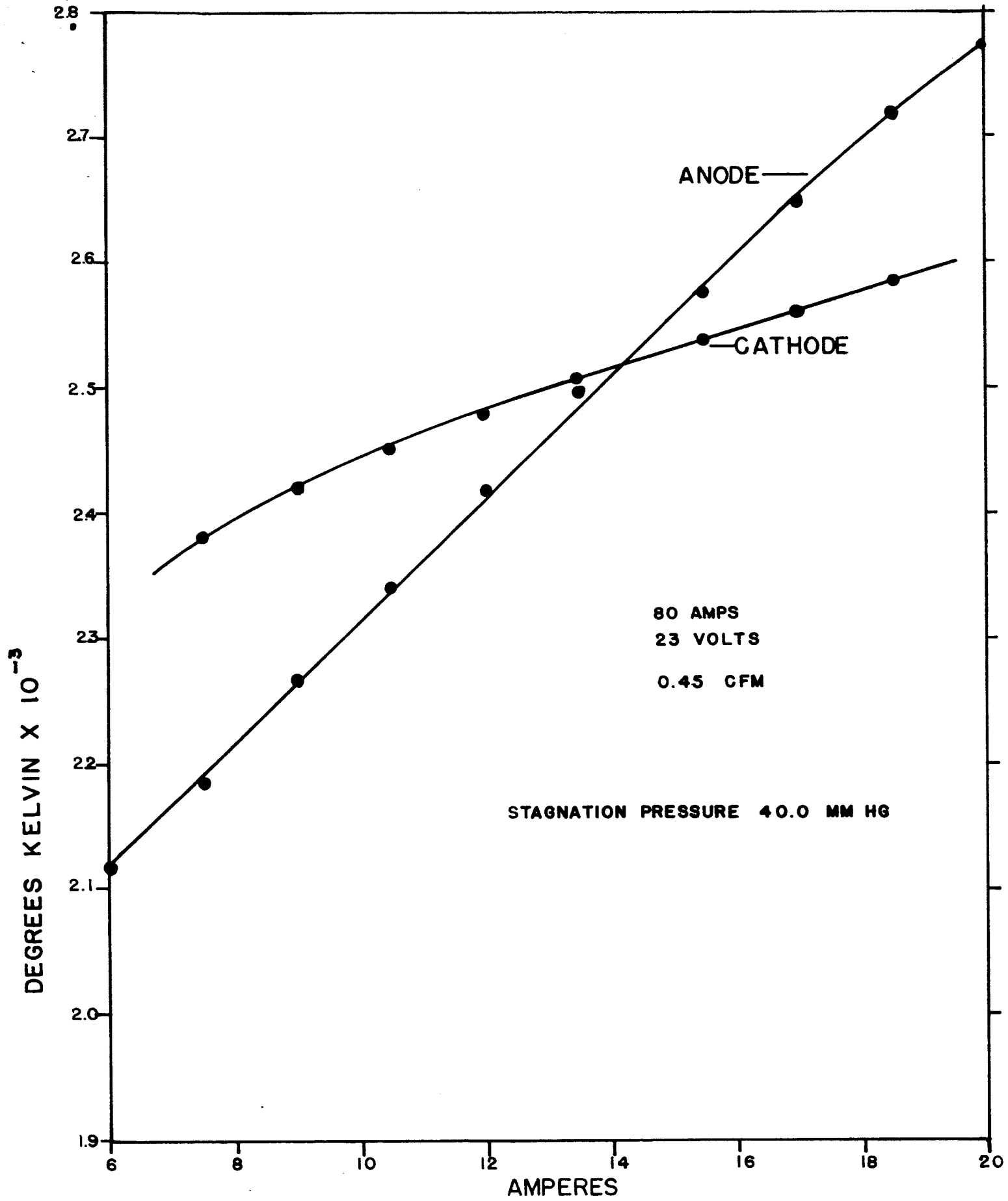
TEMPERATURE VS. CURRENT TO ELECTRODE

FIGURE 14
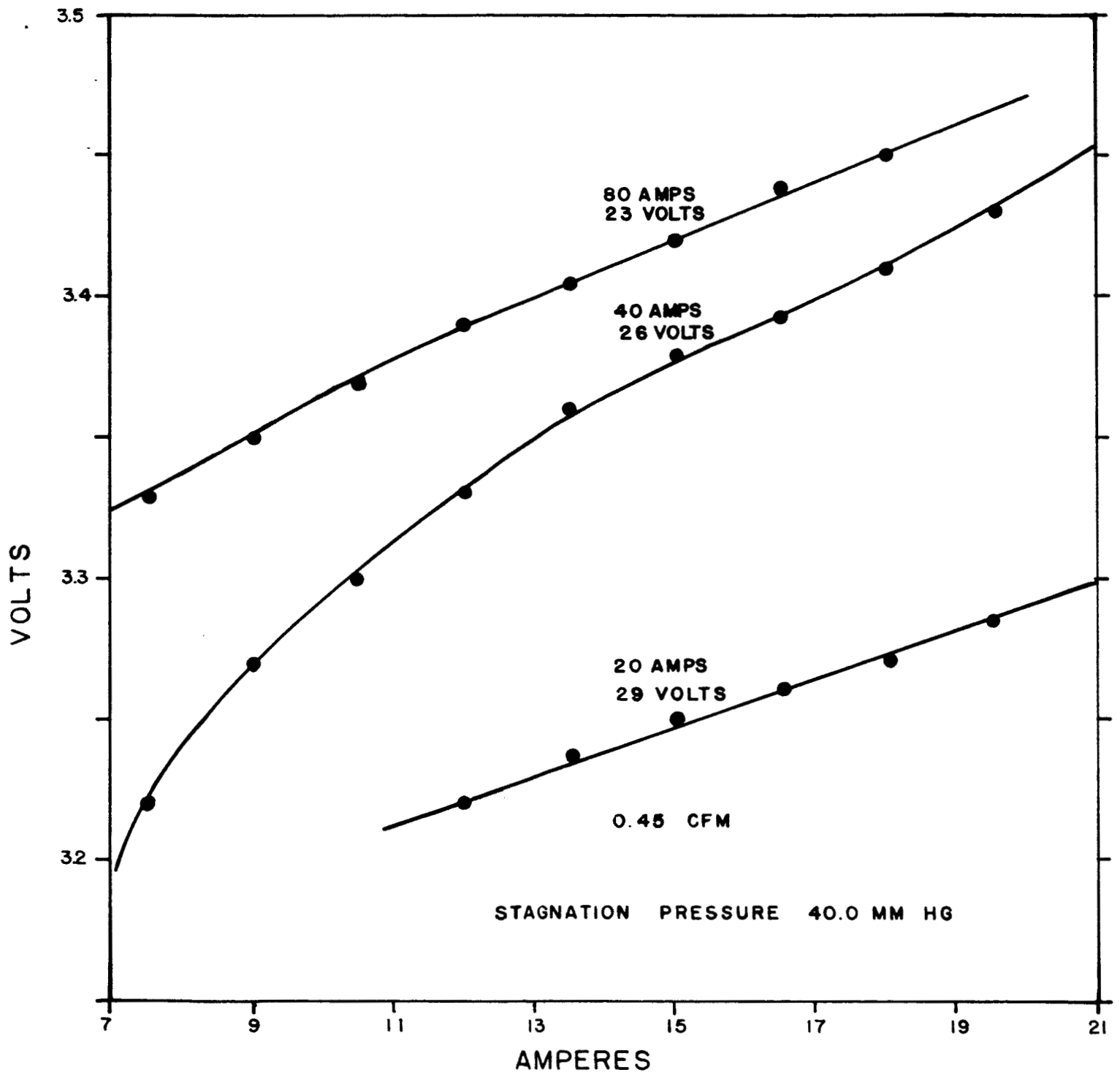
Ø FUNCTION VS. CURRENT TO ELECTRODE

FIGURE 15

$\lambda = 4259\ \overset{\circ}{A}$

40 AMPS
26 VOLTS
0.45 CFM

STAGNATION PRESSURE 40.0 MMHG
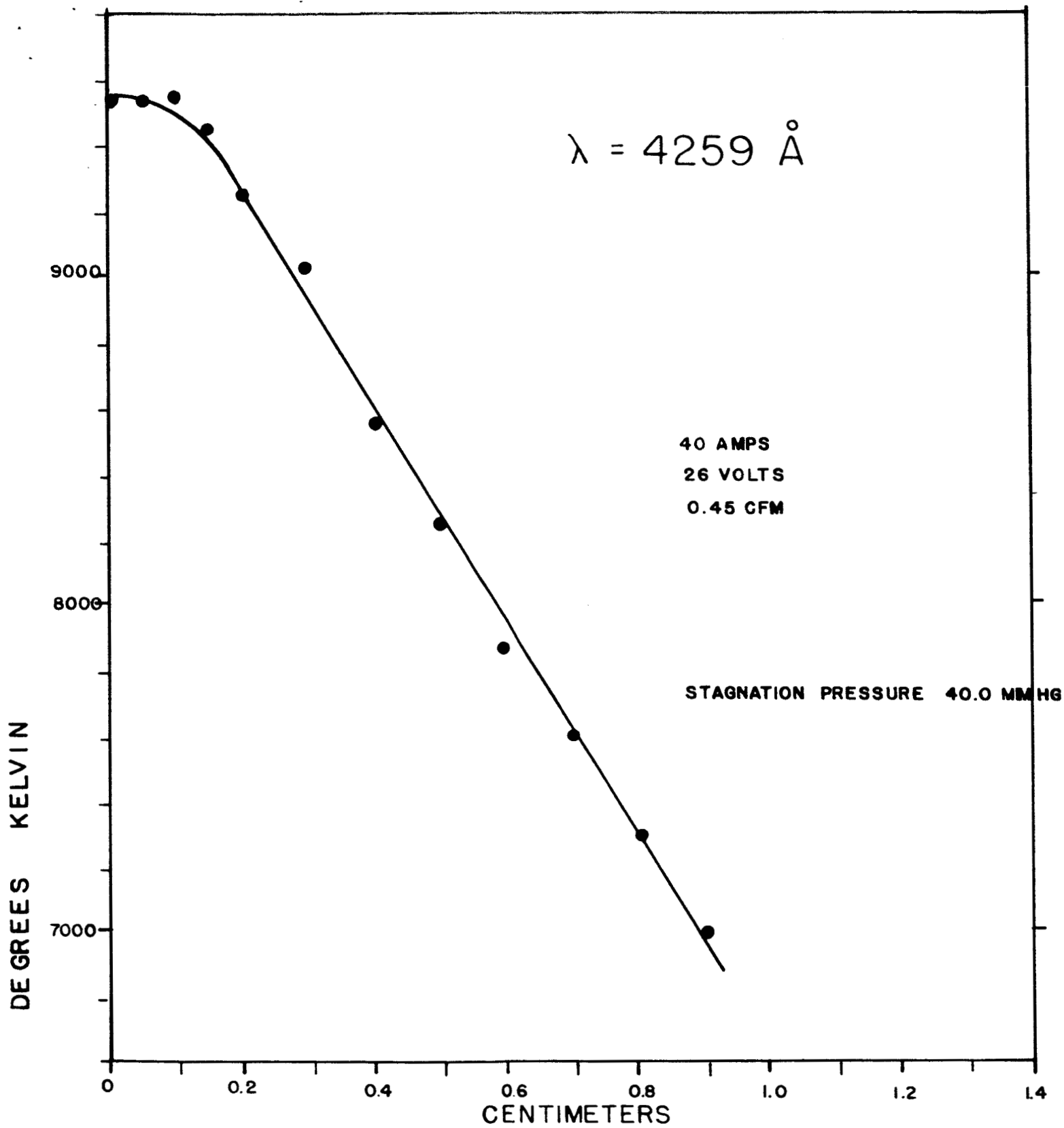
TEMPERATURE VS. RADIAL POSITION
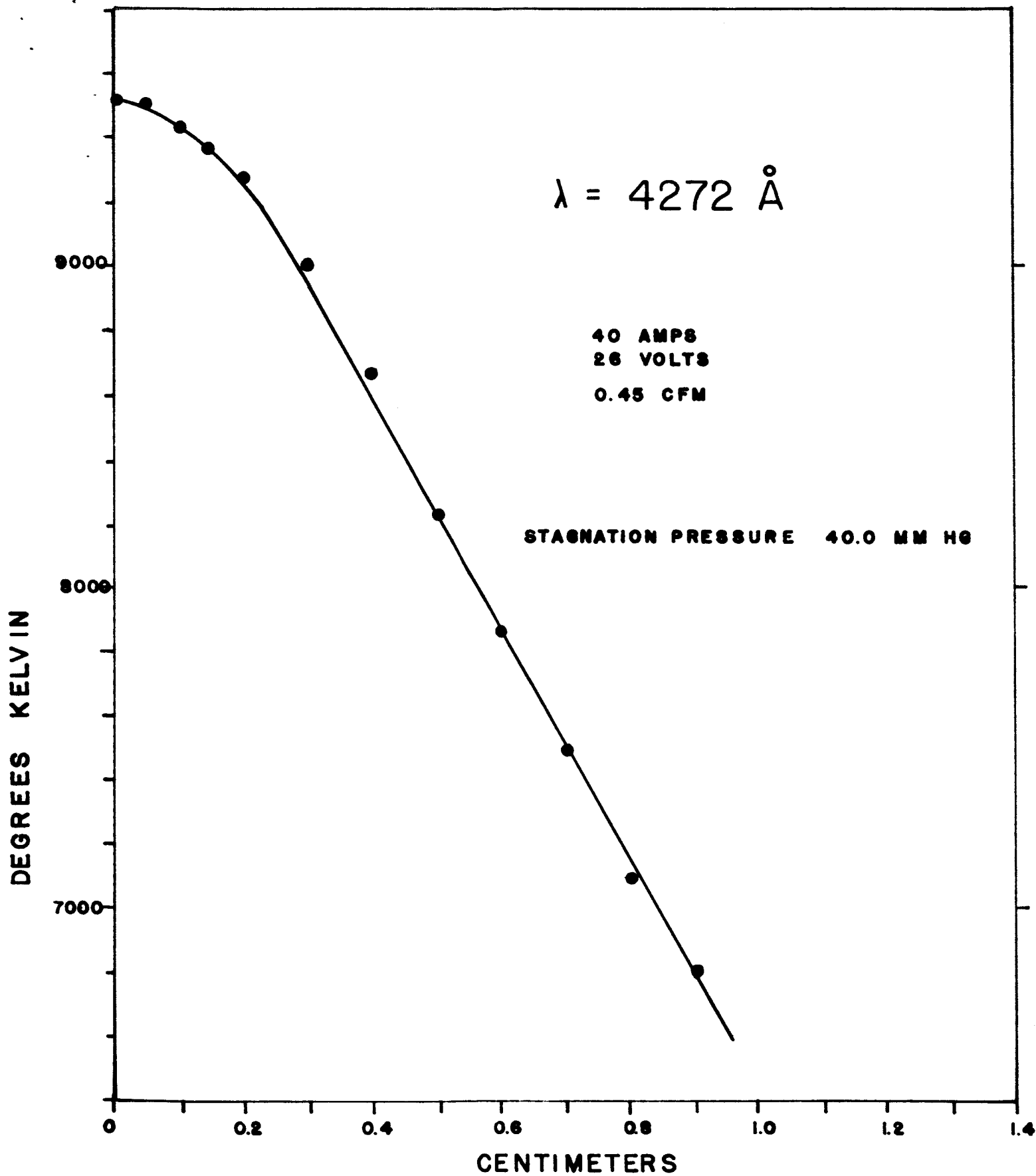
FIGURE 16

TEMPERATURE VS. RADIAL POSITION

FIGURE 17

TEMPERATURE VS. RADIAL POSITION

FIGURE 18
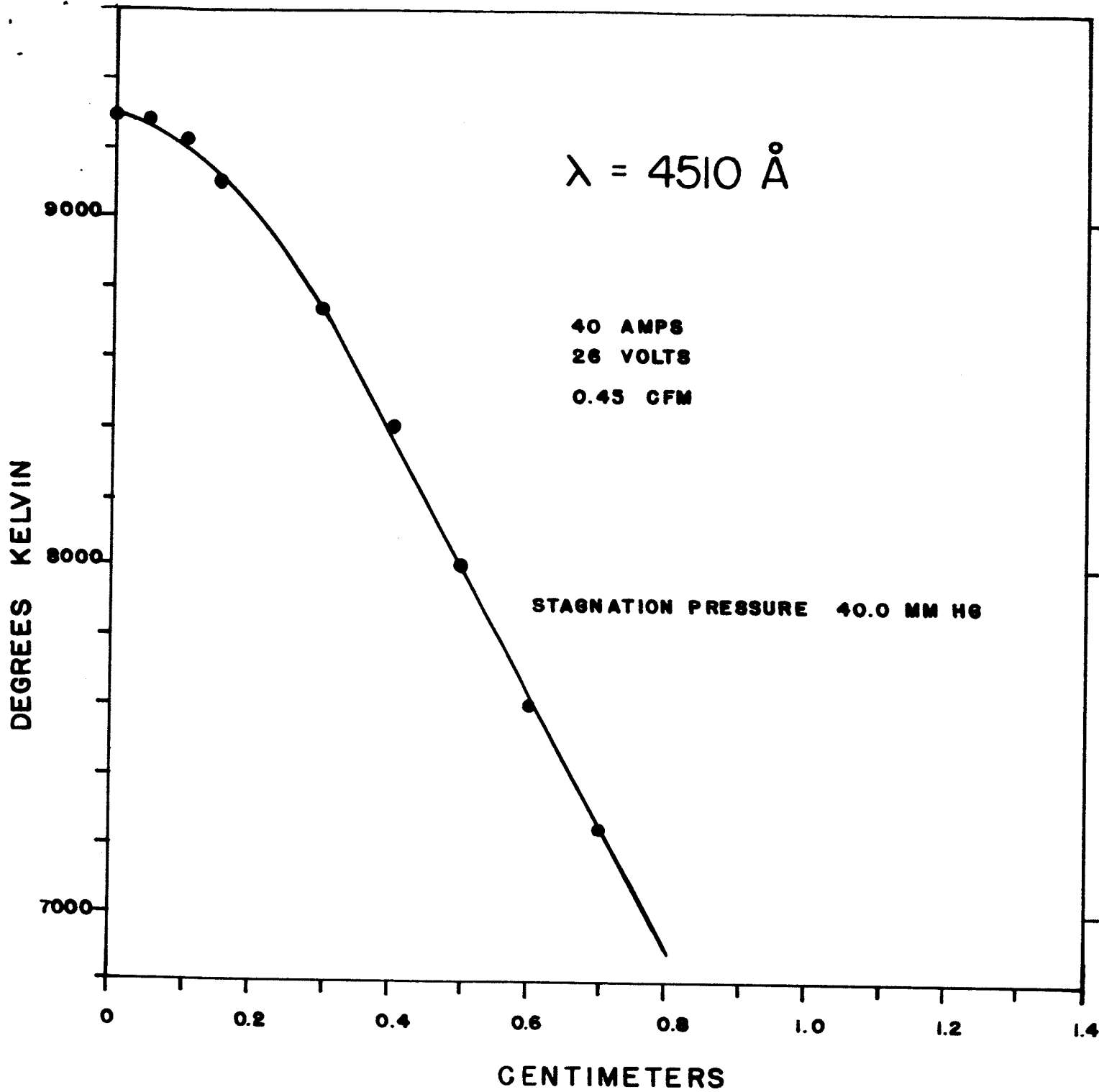
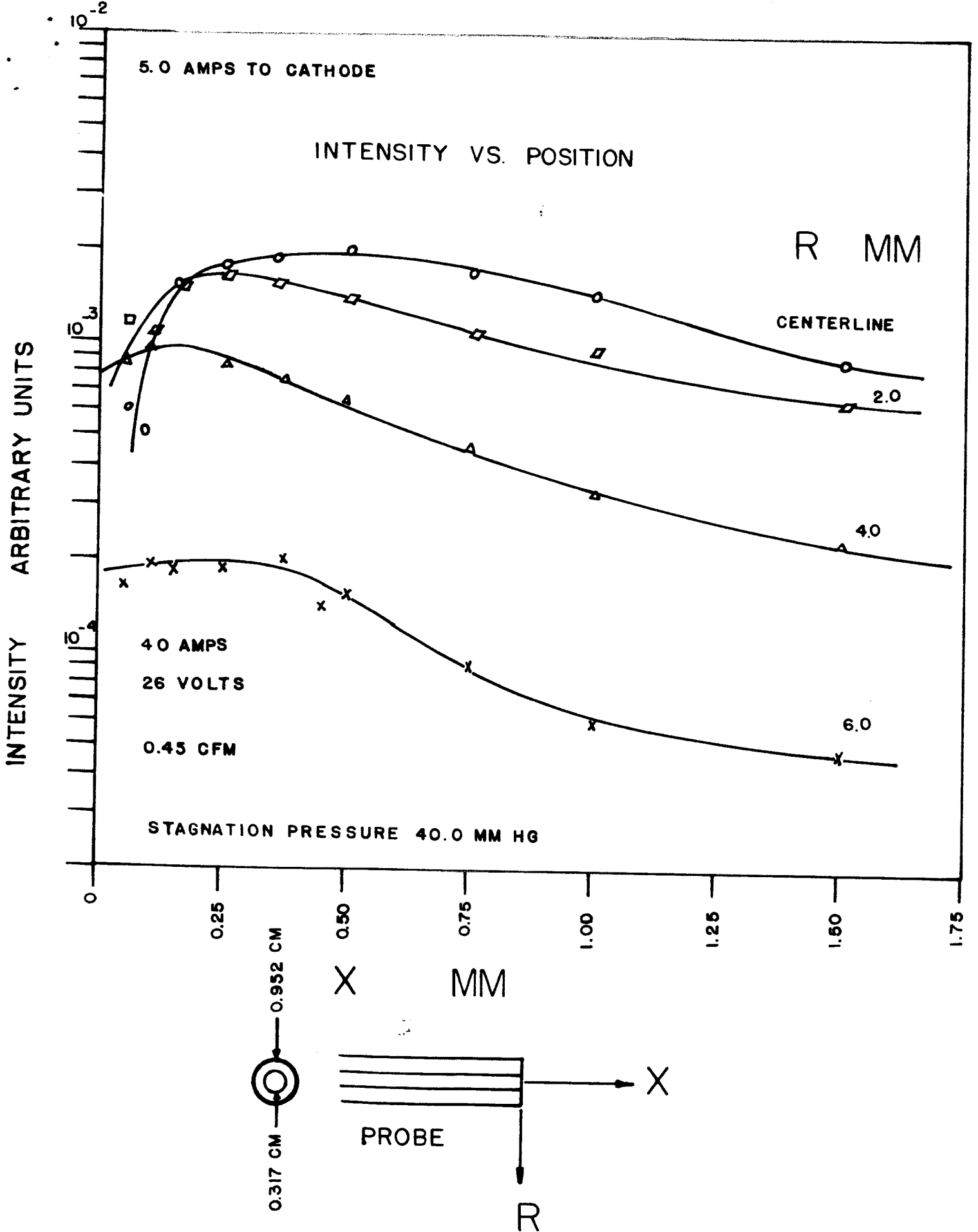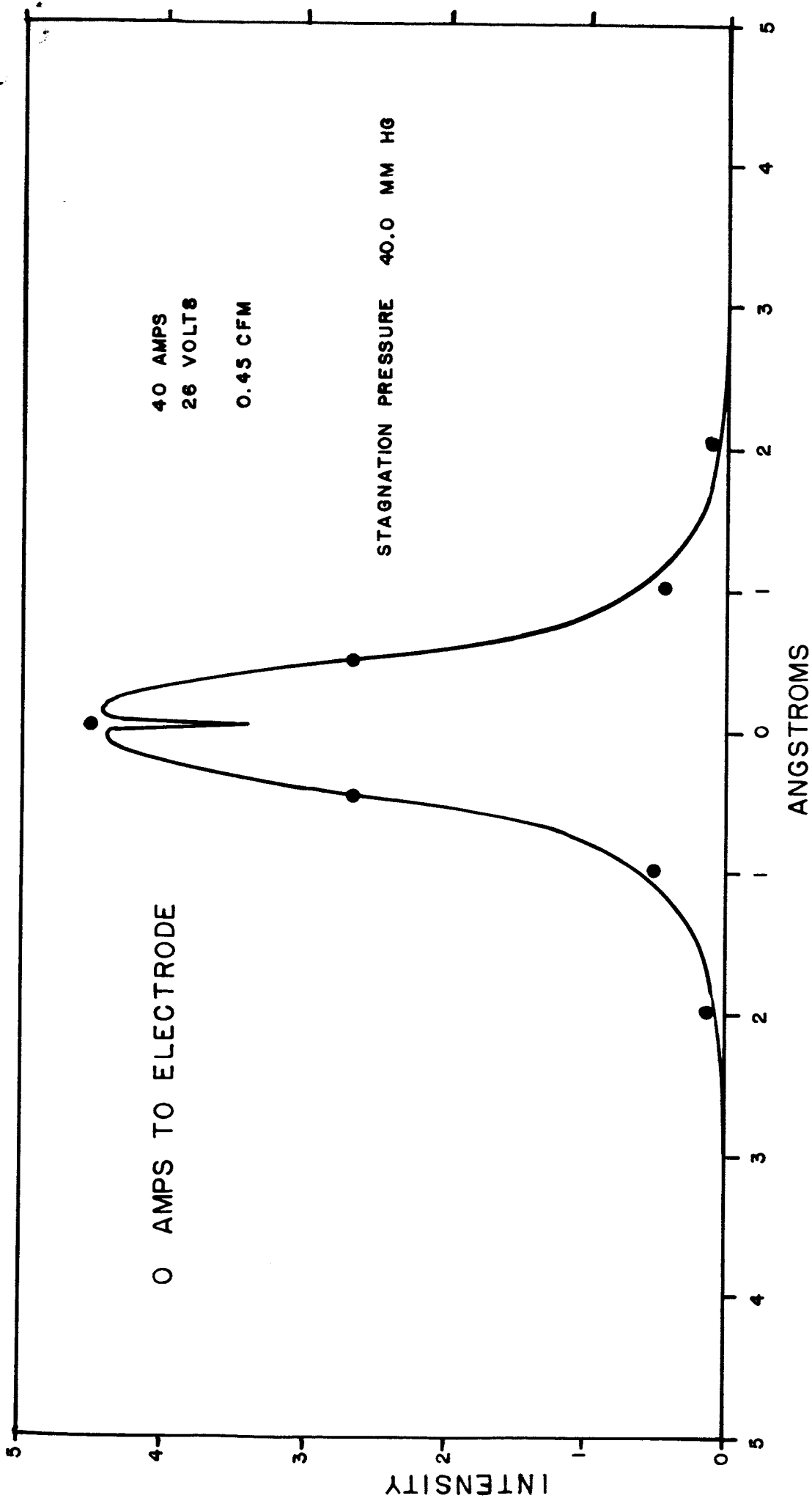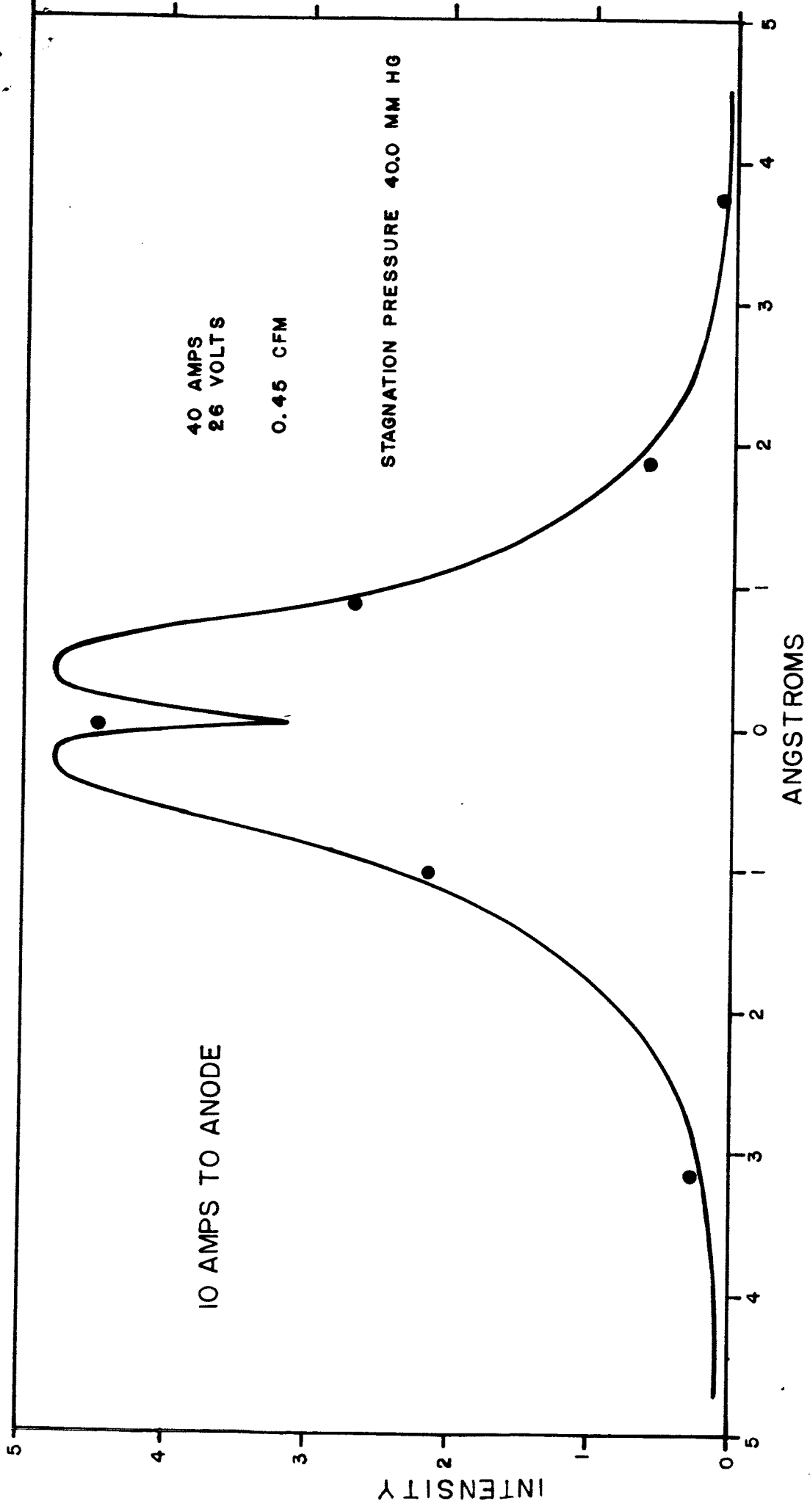TEMPERATURE VS. RADIAL POSITION
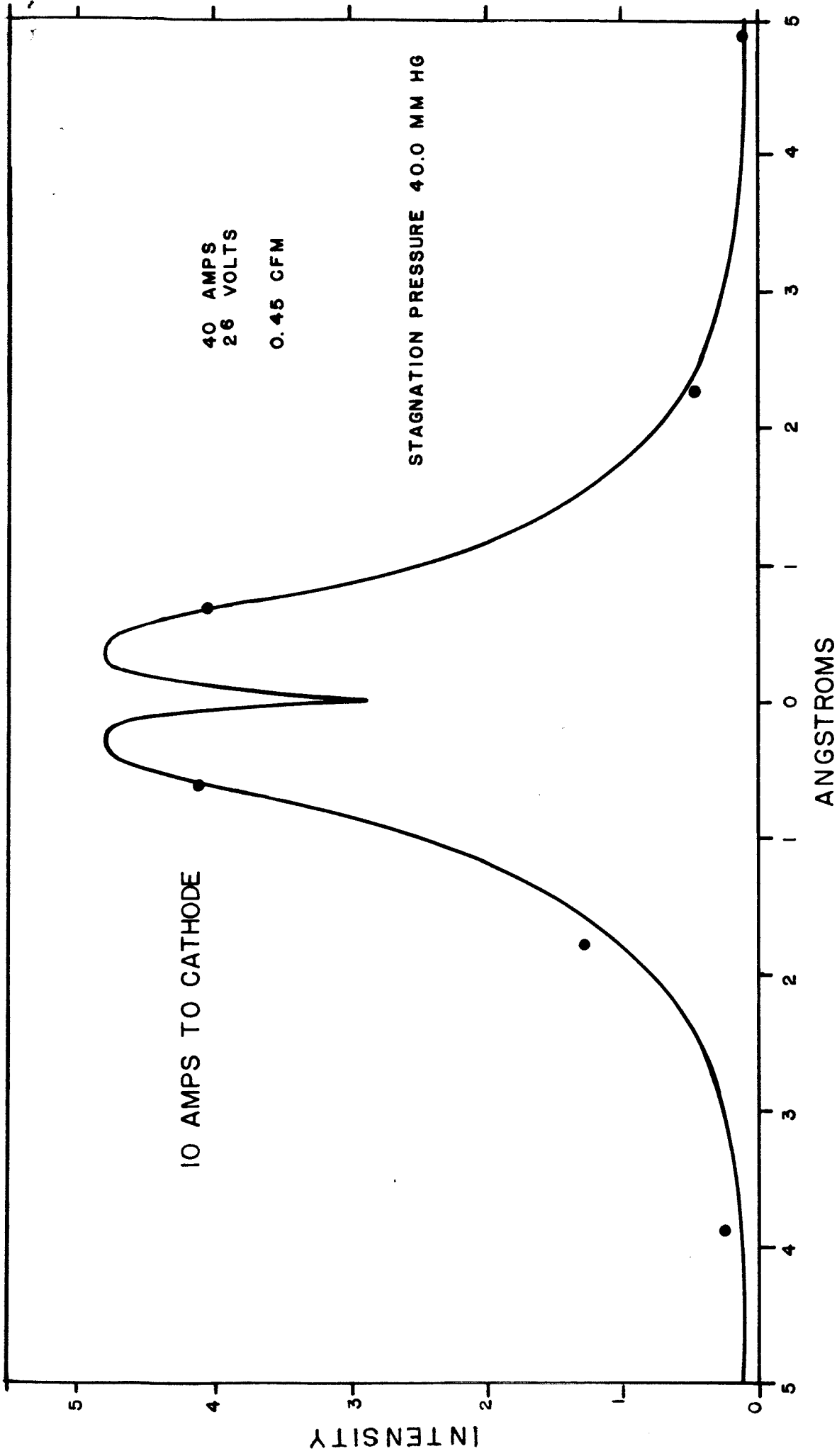
FIGURE 19

FIGURE 20

FIGURE 21

RELATIVE INTENSITY VS. Δ λ

FIGURE 22

RELATIVE INTENSITY VS. Δλ

10 AMPS TO CATHODE

40 AMPS
26 VOLTS
0.45 CFM

STAGNATION PRESSURE 40.0 MM HG

INTENSITY

ANGSTROMS

RELATIVE INTENSITY VS. Δ λ

FIGURE 23